

# Multi-Scale and Snakes for Automatic Road Extraction

Helmut Mayer, Ivan Laptev, Albert Baumgartner

Chair for Photogrammetry and Remote Sensing  
Technische Universität München  
D-80290 München, Germany

Phone: +49-89-2892-2688, Fax: +49-89-2809573

E-Mail: {helmut|ivan|albert}@photo.verm.tu-muenchen.de

**Abstract.** This paper proposes an approach for automatic road extraction in aerial imagery which exploits the scale-space behavior of roads in combination with geometric constrained snake-based edge extraction. The approach not only has few parameters to be adjusted, but for the first time allows for a bridging of shadows and partially occluded areas using the heavily disturbed evidence in the image. The road network is constructed after extracting crossings of various shape and topology. Reasonable results are obtained which are evaluated based on ground truth.

## 1 Introduction

Aerial imagery is one of the standard data sources to extract topographic objects like roads or buildings for geographic information systems (GIS). Road data in GIS are of major importance for applications like car navigation or guidance systems for police, fire service or forwarding agencies. As their extraction is time consuming, there is a need for automation.

For practical applications there will be, at least for some time, human interaction needed which leads to semi-automatic approaches. Approaches relying strongly on this interaction are for instance based on road tracking [15,23] starting from a given point and a given direction after extracting parallel edges or by extrapolation and matching of profiles in high resolution images. Other semi-automatic approaches are based on finding an optimal path between a few given points using for instance dynamic programming [9,16] or the F\*-algorithm [6] after detecting lines from low-resolution. When more than one image is available, it is possible to track the line in 3D which constrains the path of the road and makes it possible to handle occlusions using robust optimization [9]. So-called “ziplock snakes” [17] are another means to connect given points in the presence of obstacles. In [7] the model-based optimization of ribbon snakes networks is proposed to improve coarsely digitized road networks.

Another way to tackle the problem is to start with fully automatic extraction and manually edit the result only afterwards. This is the way taken in this paper and by many others. [24] extends [15] to fully automatic extraction by

finding starting points. [5] and [3] concentrate on how to improve road extraction using given GIS-data. One of the recent approaches which are similar to the one proposed here is [1]. It complements a low-level Markov-Random-Field model for the extraction of road seeds and the tracking of roads with a simple clutter and occlusion model and a Kalman filter. Another recent approach improves road extraction by modeling the context, i.e., other objects like shadow, car or tree hindering or supporting the extraction of the road [18,19]. A division of the context into spatially more global and more local parts is presented in [2]. In [18,19] roads in urban areas are extracted by detecting and grouping of cars. [2,22] utilize the scale-space behavior of the roads, the road network is globally optimized, intersections are modeled, and markings are used to verify the existence of the road.

This paper is an extension of [12]. Its main idea is to take advantage of the scale-space behavior of roads in combination with geometric constrained edge extraction by means of snakes. From the scale-space behavior of roads it is inferred to start with extracting lines in coarse scale which are less precise but also less disturbed by cars, shadows, etc., than features in fine scale. The lines initialize ribbon snakes in fine scale which describe the roads as bright, more or less homogeneous elongated areas. Ribbons with constant width are accepted as *salient* roads. The connections between adjacent ends of *salient* roads are checked if they correspond to *non-salient* roads. As those are disturbed, the evidence for the road in the image can only be exploited when additional constraints and a special strategy focus the extraction. The constraints are low curvature and constant width of roads as well as the connectivity of the road network, i.e., start and end point are given. The strategy is to optimize the width only after optimizing the center of the snake with the “ziplock” method.

The paper is organized as follows: In Section 2 model and inherent strategy essentially based on the scale-space behavior of roads and ribbon snakes are introduced and the terms *salient* road, *non-salient* road, and crossing are defined. While Section 3 gives basic theory for ribbon snakes Section 4 comprises the main part of the paper. The extraction of *salient* roads supplies the information needed to extract the *non-salient* roads. *Salient* as well as *non-salient* roads are linked by crossings of various shape and topology. Section 5 shows that the approach gives reasonable results for which the performance was evaluated based on ground truth. The paper is concluded with a summary in Section 6.

## 2 Model and Strategy

The appearance of roads in digital imagery depends on the sensor’s spectral sensitivity and its resolution, i.e., scale in object space. The remainder of this paper is restricted to grey-scale images, and only scale dependencies are considered. Images with various scale exhibit different characteristics of roads. In images with coarse scale, i.e., more than 2 m per pixel, roads mainly appear as lines establishing a more or less dense network. Opposed to this, in images with a

finer scale, i.e., less than 0.50 m, roads are depicted as bright, more or less homogeneous elongated areas with almost constant width and bounded curvature.

In this paper results from [14] are taken advantage of. There it is shown, that in a smoothed image (here a Gaussian scale-space [13] was used), i.e., a coarser scale, lines as defined in [21] representing road axes can be extracted in a stable manner even in the presence of background objects like tree, building, or car. Here the “scale” in object space resulting from smoothing is of first importance, as the goal is to extract objects in the real world which have specific sizes. This scale depends on the resolution of the image, the scale-space and the scale-parameter. Seen from a symbolical point of view, in the finer scale substructure of the road, i.e., a car on the road or also markings, as well as disturbances like shadows or partial occlusion are eliminated. This can be interpreted as an *abstraction*, i.e., an increase of the level of simplification and emphasis of the road. Abstraction is achieved simply by changing the scale of the image. Whereas coarse scale gives global information which is especially suited for initial detection of the road, the fine scale adds detailed information which can be used to verify and complete the road network. If the information of both levels is fused, wrong hypotheses for roads are eliminated by using the abstract coarse scale information, while integrating details from the fine scale, like the correct width of the roads. With this, the advantages of both scales are merged.

For line extraction in coarse scale [21] is a good choice, because it is formally well defined, its scale-space behavior was analyzed for roads (see above). In [2] it was combined with the following idea: The elongated areas of constant width describing roads in fine scale are extracted as parallel edges in the image using a local edge detector such as [4] in combination with grouping [20]. This has the following problems: The quality of edges varies due to noise, changes in radiometry of the road surface and its background, occlusions, etc. [8]. Therefore, the extraction of edges based on purely local photometric criteria often results in an incomplete detection of few significant edges or in the detection of many irrelevant edges. When these edges are grouped into parallelograms, they tend to be fragmented, even when lines from coarse scale are used in the grouping process and help to eliminate many wrong hypotheses. When parallel edges are linked based on purely geometric criteria, the precision is poor and wrong hypotheses are common [2].

Opposed to this, the framework of snakes introduced in [11] gives the possibility to focus the extraction of edges by their priori known geometric properties. Here this is done by linking two edges into a “ribbon” defined by its center and its width. The ribbon is optimized using the idea of “snakes” [11] which leads to the so-called “ribbon snakes”. Based on the scale-space behavior and the ribbon snakes, the model and the inherent “hypothesize and verify” strategy for the extraction of the road network are as follows:

- ***Salient roads*** have a distinctive appearance in the image. A line from coarse scale initializes the center of a ribbon snake in fine scale. Criteria for the verification of a *salient* road are the constancy of the width and the homogeneity of the corresponding image region. Since man-made objects

such as houses have similar properties, the extraction of *salient* roads is restricted to rural areas, given by a GIS or segmented by means of texture features. This is similar to [2], where the “context regions” *suburb\_urban*, *forest*, and *open\_rural* are introduced and the extraction of roads is restricted to the latter ones.

- **Non-salient roads** correspond to parts of the road network which are in the image more or less disturbed by shadows or partial occlusions. They can only be extracted top-down, when a start and an end point are available. This exploits the fact that all roads are connected into a global network. Taking adjacent ends of *salient* roads as start and end point, these points are connected by a ribbon snake with fixed width using the “ziplock” method. After a subsequent optimization of the width, its constancy is used for the verification of the *non-salient* roads.
- **Crossings** link the road network together. In coarse scale they correspond to the junctions from line extraction [21]. These hypotheses for crossings are verified in fine scale by expanding a closed snake around each junction and checking the connections between the crossings’ outline and adjacent roads.

### 3 Ribbon Snakes

The original snakes introduced in [11] are curves with a parametric representation whose position is optimized under a number of constraints. On the one hand, the photometric constraints evoke the *image* forces which “pull” the snake to features in the image. On the other hand, the geometric constraints give rise to the *internal* forces which control the shape of the snake ensuring its piecewise smoothness. During optimization the snake evolves from its initial position to a position where the forces compensate each other and the energy of the snake is minimized. This state implies that the snake is located at the image features which best of all satisfy the desired properties.

For road extraction the original snakes are extended with a width component [7] leading to a ribbon snake defined as:

$$\mathbf{v}(s, t) = (x(s, t), y(s, t), w(s, t)), \quad (0 \leq s \leq 1), \quad (1)$$

where  $s$  is proportional to the ribbon’s length,  $t$  is the current time,  $x$  and  $y$  are the coordinates of the ribbon’s centerline, and  $w$  is the ribbon’s half width. As shown in Figure 1(a) the centerline  $(x(s, t), y(s, t))$  and its width  $w(s, t)$  define the sides of the ribbon  $\mathbf{v}_L(s, t)$  and  $\mathbf{v}_R(s, t)$ . Using this representation, the original expression for the snake’s *internal* energy still holds and the width is constrained by the same “tension” and “rigidity” forces as the two coordinate components. Differently from snakes, the image forces for ribbon snakes are considered along the sides. When optimizing a ribbon to a bright road on a dark background the image function  $P$  can be redefined as the sum of the magnitudes of the image gradient along the curves  $\mathbf{v}_L(s, t)$  and  $\mathbf{v}_R(s, t)$ . An even better way is to use the projections of the image gradient onto the ribbon’s normal  $\mathbf{n}(s, t)$  constraining them to be positive at the ribbon’s left side and negative at its right

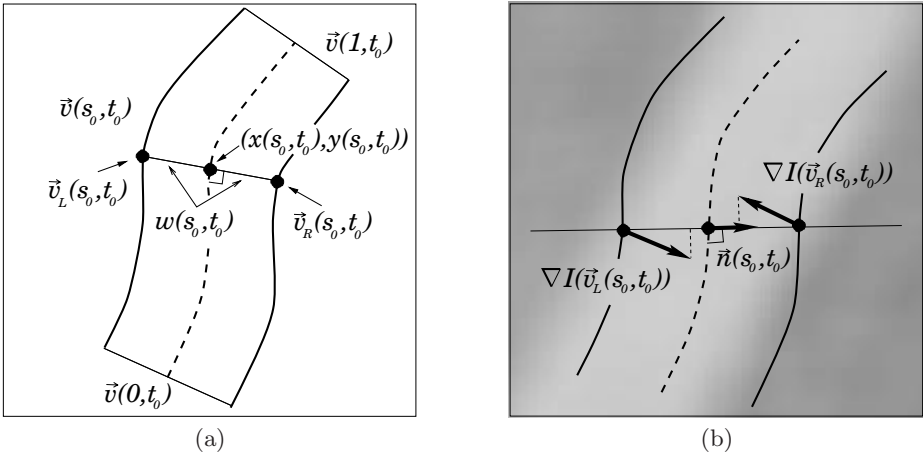


**Fig. 1.** (a) Parametric representation of the ribbon snake. Each slice of the ribbon  $\mathbf{v}(s_0, t_0)$  is characterized by its center  $(x(s_0, t_0), y(s_0, t_0))$  and width  $w(s_0, t_0)$ . Center and width define points  $\mathbf{v}_L(s_0, t_0)$  and  $\mathbf{v}_R(s_0, t_0)$  corresponding to the left and right side of the ribbon. (b) Image gradients for the left and the right side and their projection to the ribbon's unit normal vector  $\mathbf{n}(s_0, t_0)$ .

side (cf. Figure 1(b)). By this means the correspondence between the road sides and the sides of the ribbon is obtained. Using

$$P(\mathbf{v}(s, t)) = (\nabla I(\mathbf{v}_L(s, t)) - \nabla I(\mathbf{v}_R(s, t))) \cdot \mathbf{n}(s, t) \tag{2}$$

for the image function, the expression for the total energy of the ribbon snakes remains identical with the correspondent formula for the energy of the original snake:

$$E(\mathbf{v}) = - \int_0^1 P(\mathbf{v}(s, t)) ds + \frac{1}{2} \int_0^1 \alpha(s) \left| \frac{\partial \mathbf{v}(s, t)}{\partial s} \right|^2 + \beta(s) \left| \frac{\partial^2 \mathbf{v}(s, t)}{\partial s^2} \right|^2 ds. \tag{3}$$

The first term of equation (3) represents the *image* energy and the second corresponds to the *internal* energy.  $\alpha(s)$  and  $\beta(s)$  are arbitrary functions which determine the influence of the geometric constraints on the optimization.

The application of the ribbon snakes to fully-automatic extraction requires that the balance between their *image* and *internal* energies has to be achieved automatically. Assuming the initial estimate of the ribbon to be close to the final solution, this can be enforced by substituting the functions  $\alpha(s)$  and  $\beta(s)$  in (3) with a factor  $\lambda$  [8]:

$$\lambda = \frac{|\delta E_{img}(\mathbf{v})|}{|\delta E_{int}(\mathbf{v})|}, \tag{4}$$

where  $\delta$  is the variational operator. This simplification avoids the manual adjustment of  $\alpha(s)$  and  $\beta(s)$ . What is also important for the extraction is the ability

to restrict and control the ribbon's motion during optimization. For this reason it is a good idea to "embed" the ribbon in a viscous medium and obtain the solution by minimizing the term  $\int E(\mathbf{v}) + D(\mathbf{v})dt$ , where  $D$  is the dissipation functional  $D(\mathbf{v}) = \frac{1}{2} \int_0^1 \gamma(s) |\mathbf{v}_t|^2 ds$  with the damping coefficient  $\gamma$ . As shown in [8] the derivation of  $\gamma$  from

$$\gamma = \frac{\sqrt{2n}}{\Delta} \left| \frac{\partial E(\mathbf{v})}{\partial \mathbf{v}} \right| \quad (5)$$

ensures that the displacement of each vertex of the ribbon during one optimization step is on average of magnitude  $\Delta$ . This property has shown to be very useful for automatic road extraction since changing the  $\Delta$ , the search space for the hypothetical road sides can be directly controlled by a higher level program.

## 4 Road Extraction

### 4.1 Extraction of *Salient* Roads

According to model and strategy in Section 2, the first step is the extraction of lines in coarse scale [21]. However, as shown in Figure 2(a), there can be many other features with properties similar to roads which will be extracted as well. In order to separate them from the roads, i.e., to verify the roads, more evidence is required. In fine scale it is possible to determine the precise width of the structure corresponding to the line in coarse scale. Thresholding the variation of width along each hypothesis, irrelevant structures can mostly be eliminated since their width is much more unstable than the width of roads.

Following this idea the boundaries of the structures corresponding to the lines in coarse scale are extracted with ribbon snakes. For each detected line a ribbon is optimized. The initial position of the ribbons' centerlines coincide with the lines and the width is set to 0. In order to obtain a rough approximation of the searched boundaries the ribbons are firstly optimized in the images of coarse scale. Later, re-optimization in fine scale is performed to delineate the details of the boundaries. During optimization the width of the ribbons is expanded to ensure, that the sides of wide objects will be extracted as well.

As can be seen in Figure 2(b) the optimized ribbons which correspond to wrong road hypotheses have a stronger variation of width than the ribbons optimized at *salient* roads. Thus, thresholding the standard deviation of width for the short pieces of ribbons enables selection of ribbon's parts which correspond to roads with high probability (cf. Figure 2(c)).

### 4.2 Extraction of *Non-Salient* Roads

Typical reasons for gaps between *salient* roads are shadows or partial occlusions (cf. Section 2). To bridge the gaps, two adjacent ends of *salient* roads are connected with a road hypothesis which is then verified based on homogeneity and

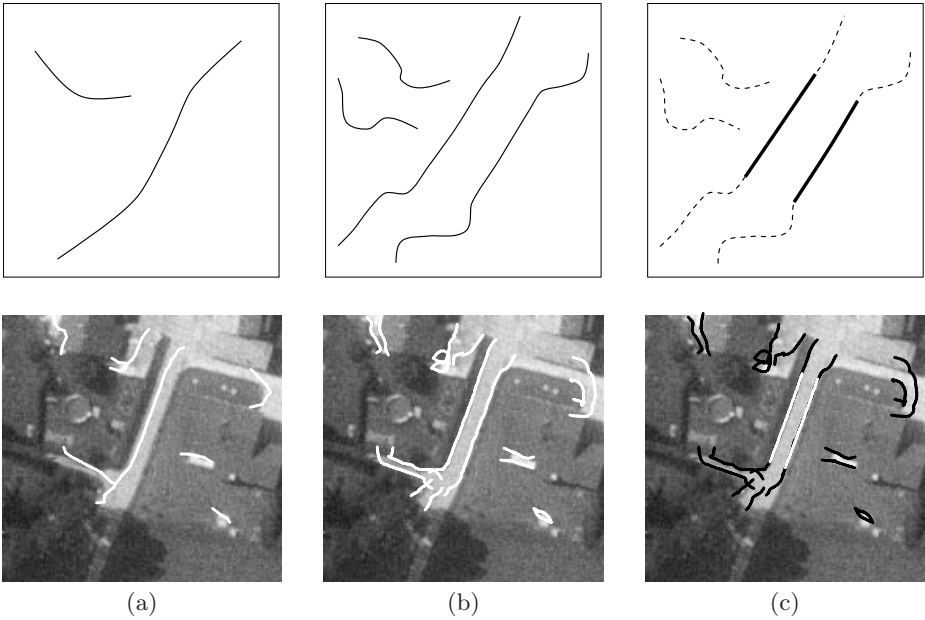


**Fig. 2.** Extraction of *salient* roads. (a) Extraction of lines (b) Optimization of ribbons' boundaries (c) Selection of ribbons' parts with constant width. Only the white ribbon is accepted as a correct hypothesis for a *salient* road.

the constancy of width (cf. Figure 3). The regions corresponding to the gaps show in many cases at least one traceable road side, although they may contain many other irrelevant edges which potentially disturb road extraction. However, as shown in Figure 3(a), the curvature of these edges is mostly much higher than the curvature of the road sides.

For each hypothesis a ribbon snake is initialized with its position, direction and width at its ends corresponding to the position, direction, and width at the end points of the adjacent *salient* roads (cf. Figure 4(a)). Since the initial approximation of the ribbon's centerline can be far away from the road's correct centerline, the optimization uses the "ziplock" method [17]. "Ziplock" method means that the information is gradually propagated from the ribbon's ends toward its center by optimizing only parts of the snake at a time while approaching the center. The curvature of the ribbon is constrained to be low. By this means, the "active" parts of the ribbon remain close to the road sides during the whole optimization (cf. Figure 4). At this point only the centerline of the ribbon is optimized and the width is fixed and equal to the average width of the *salient* roads at the ribbon's ends. Note, that due to the choice of the image function  $P$  in equation (2), the ribbon is insensitive to edges which cross perpendicular to its direction. This property is important because shadows and occlusions often

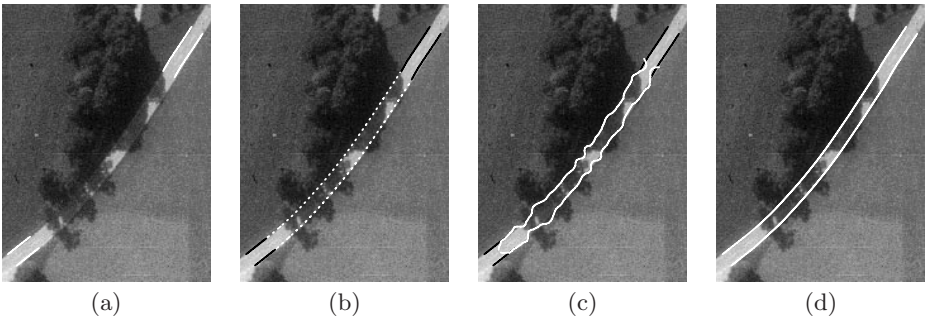


**Fig. 3.** Extraction of *non-salient* roads. (a) Selection of initial hypothesis (b) Extraction of optimal path; (c) Verification by optimization of width (d) Selection of hypothesis with constant width

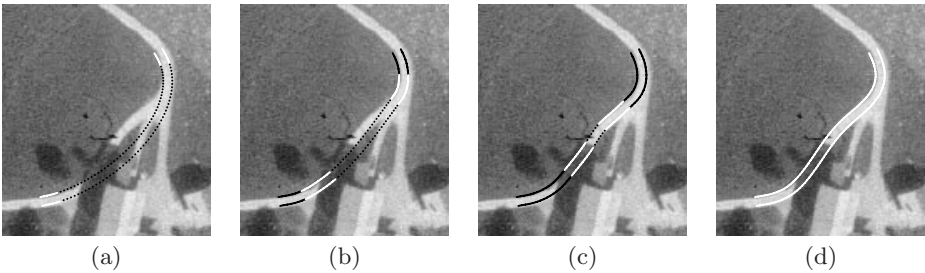


**Fig. 4.** Steps of the optimization of a “ziplock” ribbon. (a)-(c) Dotted lines indicate the passive part of the ribbon. White parts are currently optimized. Black ends indicate the result of the optimization so far. (d) Final result

result in this kind of edges. At the same time even weak contrast of road sides attracts the ribbon and supports correct road extraction.

Because it is not clear at this point which connections of adjacent ends of *salient* roads correspond to roads, there will always be wrong hypotheses. This implies that the result obtained in Figure 4(d) has to be verified. The verification is performed in two steps. Firstly, the homogeneity of the region in the image which corresponds to the ribbon is checked and ribbons with low variation of the image intensity are accepted as *non-salient* roads. This, however, will reject most of the shadowed and occluded roads and therefore a second step is taken: The centerlines of the ribbons are fixed and only the width is expanded and optimized. As shown in Figures 5(a,b), given a correctly located road hypothesis, the fixed centerline together with the contrast on one road side stops the expansion of the width at the right place. However, random features localized close to wrong hypotheses will in most cases result in a large variation of the width (cf. Figure 5(c,d)). This implies that wrong hypotheses can be rejected based on their high variation of the width.

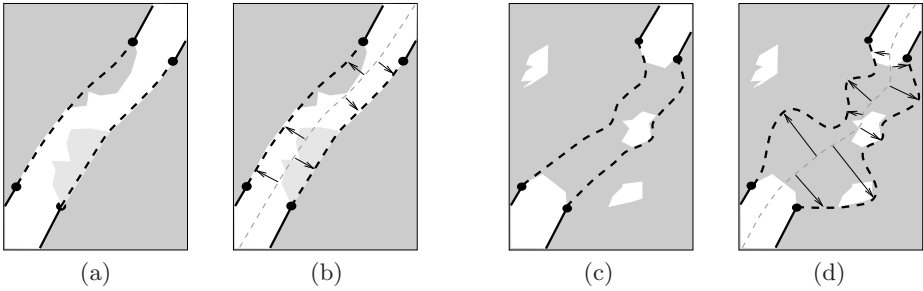


**Fig. 5.** Verification of hypotheses by expanding the width (a),(b) Verification of correct hypothesis. Since the ribbon’s centerline in (b) is fixed, the contrast at only one side is enough to stop the expansion (c),(d) Verification of wrong hypothesis. Random features result in a big variation of the width (d).

### 4.3 Extraction of Crossings

The extraction of crossings is complicated since the variability of their shape makes it difficult to distinguish them from other objects. However, as shown below, the *salient* and *non-salient* roads greatly help to reduce the search-space.

In order to generate initial hypotheses for crossings, two observations are taken advantage of:

- During the extraction of *non-salient* roads most of the gaps in *salient* roads caused by crossings will be bridged (cf. Figure 4(d) and 6(a)).
- As exemplified in Figures 2(a) and 8(a), line extraction often results in junctions inside crossings. However, a big number of such junctions corresponds to irrelevant features.

Combining these two observations, crossings are hypothesized at junctions which are adjacent to previously extracted roads (cf. Figure 6(a)). Next, the outline of the crossing is approximated. A closed snake is initialized around the junction, its contour is expanded and optimized (cf. Figures 7(a)-(c), 6(b)). Based on this, as shown in Figure 6(c), the connections between the crossing and adjacent ends of roads are established and verified using the method of the previous Section. Finally, the crossing is accepted if at least one of the adjacent roads can be connected to it (cf. Figures 6(d), 7(d)).

The advantage of the chosen strategy is that it does not make restricting assumptions about the shape and the topology of the crossings. Therefore, crossings with different size connecting a varying number of roads can be extracted.

## 5 Results and Their Evaluation

Although the approach was developed for rural areas, a successful recognition is in some cases possible also in built-up areas (cf. Figure 8). As presented in

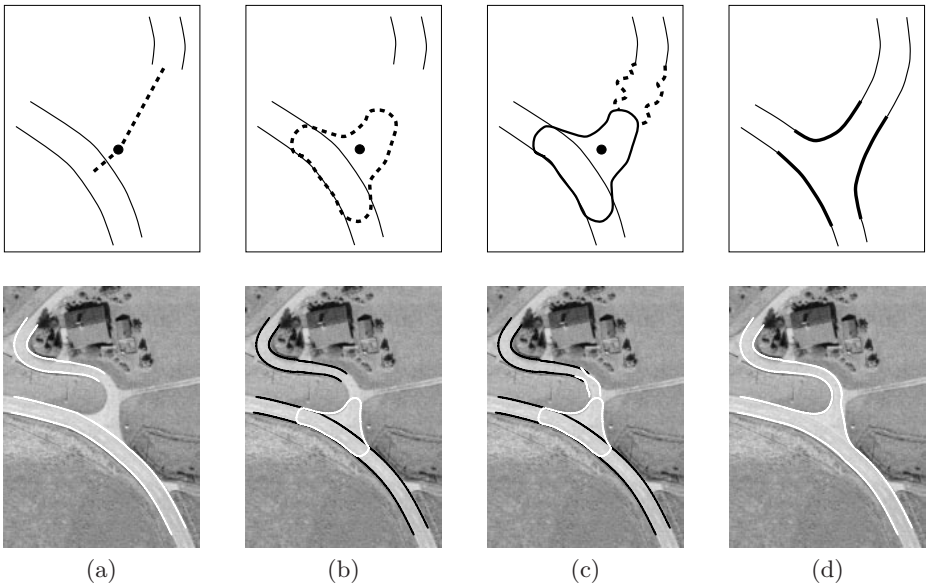


**Fig. 6.** Extraction of crossings (a) Selection of initial hypothesis (b) Approximation of the crossing's outline (c) Verification of connections to adjacent roads (d) Construction and connection of the crossing

Figure 8(a), line extraction alone will in most cases not detect all roads and can result in more wrong hypotheses than correct ones. However, using the proposed approach, all wrong hypotheses are eliminated and additionally gaps caused by shadows are bridged (cf. Figure 8(b)). Figure 9 shows the result for a larger scene. As can be seen, most of the roads are correctly delineated and connected into a network by the crossings. An evaluation of the results according to [10] is shown in Table 1 for the previous and two other images. The evaluation is based on the comparison of the extracted road centerlines to ground truth, i.e., manually plotted road axes used as reference. Figure 9 is a part of the image “Erquy”, which can be described as “flat, agricultural, difficult”, whereas the image “Marchetsreut” is “flat, agricultural, easy”.

The “correctness” in Table 1 represents the ratio of the length of correctly extracted roads to the length of all extracted roads. The values prove that only a small number of false roads is extracted. “Completeness” corresponds to the ratio of the length of the correctly extracted roads and the length of the reference roads. Though the values for completeness are quite high for an automatic approach, they could have been even higher if forest and urban areas, where contrast on both road sides is weak, had been excluded from evaluation. The RMS values show that the precision is high and, most important, much better than demanded in most standards for topographic objects in GIS. For all three examples they are better than one pixel and close to the value which arises from

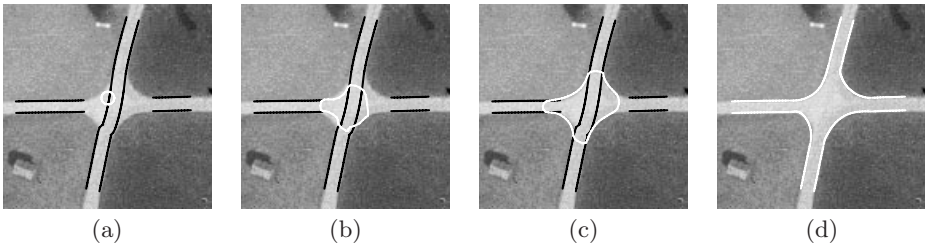


**Fig. 7.** Steps of the optimization of a crossing's outline (a) Initial state of the closed snake (b),(c) 10th and 20th step (d) Final result.

	Figure 9	Erquy	Marchetsreut
Correctness	0.97	0.95	0.99
Completeness	0.83	0.72	0.84
RMS [m]	0.46	0.46	0.37
Image size [pixel]	1800 · 1600	4500 <sup>2</sup>	2000 <sup>2</sup>
Time [min]	18	80	15

**Table 1.** Evaluation of results obtained by snake-based road extraction in images with a resolution of  $0.5m$

the fuzzy definition of the road sides. The time for the extraction (Sun Sparc 20) is reasonable. It is mostly proportional to the size of the image. However, it also depends on the scene and the number of roads, or more specifically, lines in it. The more gaps there are due to shadows and other disturbances in the *salient* roads, the more time it takes to verify all probable connections during the extraction of the *non-salient* roads.

## 6 Outlook

This paper shows how by using snakes it is possible to take advantage of the little evidence in shadowed parts of the road or when one side of the road is occluded. This overcomes some of the problems of the recent approaches for road extraction. Nevertheless, the proposed approach is mostly restricted to rural areas. Therefore, the best idea would be to combine it with the assets of other approaches. These are particularly the modeling of the context in [2] or [18], the extraction of groups of cars to extract roads in urban areas of [19] and the use of GIS information in [3].

## Acknowledgments

We would like to thank Wolfgang Eckstein, Tony Lindeberg, Carsten Steger, and Christian Wiedemann for many fruitful discussions.



**Fig. 8.** Road extraction for a complicated scene (a) Line extraction (b) Final result

## References

1. M. Barzohar, M. Cohen, I. Ziskind, and D.B. Cooper. Fast Robust Tracking of Curvy Partially Occluded Roads in Clutter in Aerial Images. In *Automatic Extraction of Man-Made Objects from Aerial and Space Images (II)*, pages 277–286, Basel, Switzerland, 1997. Birkhäuser Verlag. [721](#)
2. A. Baumgartner, C. Steger, H. Mayer, and W. Eckstein. Multi-Resolution, Semantic Objects, and Context for Road Extraction. In *Semantic Modeling for the Acquisition of Topographic Information from Images and Maps*, pages 140–156, Basel, Switzerland, 1997. Birkhäuser Verlag. [721](#), [721](#), [722](#), [722](#), [723](#), [730](#)
3. G. Bordes, G. Giraudon, and O. Jamet. Road Modeling Based on a Cartographic Database for Aerial Image Interpretation. In *Semantic Modeling for the Acquisition of Topographic Information from Images and Maps*, pages 123–139, Basel, Switzerland, 1997. Birkhäuser Verlag. [721](#), [730](#)
4. J. Canny. A Computational Approach to Edge Detection. *IEEE Transactions on Pattern Analysis and Machine Intelligence*, 8(6):679–698, 1986. [722](#)
5. M. de Gunst and G. Vosselman. A Semantic Road Model for Aerial Image Interpretation. In *Semantic Modeling for the Acquisition of Topographic Information from Images and Maps*, pages 107–122, Basel, Switzerland, 1997. Birkhäuser Verlag. [721](#)
6. M.A. Fischler, J.M. Tenenbaum, and H.C. Wolf. Detection of Roads and Linear Structures in Low-Resolution Aerial Imagery Using a Multisource Knowledge Integration Technique. *Computer Graphics and Image Processing*, 15:201–223, 1981. [720](#)
7. P. Fua. Model-Based Optimization: Accurate and Consistent Site Modeling. In *International Archives of Photogrammetry and Remote Sensing*, volume (31) B3/III, pages 222–233, 1996. [720](#), [723](#)
8. P. Fua and Y.G. Leclerc. Model Driven Edge Detection. *Machine Vision and Applications*, 3:45–56, 1990. [722](#), [724](#), [725](#)
9. A. Grün and H. Li. Linear Feature Extraction with 3-D LSB-Snakes. In *Automatic Extraction of Man-Made Objects from Aerial and Space Images (II)*, pages 287–298, Basel, Switzerland, 1997. Birkhäuser Verlag. [720](#), [720](#)
10. C. Heipke, H. Mayer, C. Wiedemann, and O. Jamet. Evaluation of Automatic Road Extraction. In *International Archives of Photogrammetry and Remote Sensing*, volume (32) 3-2W3, pages 47–56, 1997. [729](#)



**Fig. 9.** Road extraction in larger image

11. M. Kass, A. Witkin, and D. Terzopoulos. Snakes: Active Contour Models. *International Journal of Computer Vision*, 1(4):321–331, 1987. 722, 722, 723
12. I. Laptev. Road Extraction Based on Snakes and Sophisticated Line Extraction. Master thesis, Computational Vision and Active Perception Lab (CVAP), Royal Institute of Technology, Stockholm, Sweden, 1997. 721
13. T. Lindeberg. *Scale-Space Theory in Computer Vision*. Kluwer Academic Publishers, Boston, USA, 1994. 722
14. H. Mayer and C. Steger. Scale-Space Events and Their Link to Abstraction for Road Extraction. *ISPRS Journal of Photogrammetry and Remote Sensing*, 53:62–75, 1998. 722
15. D.M. McKeown and J.L. Denlinger. Cooperative Methods For Road Tracking In Aerial Imagery. In *Computer Vision and Pattern Recognition*, pages 662–672, 1988. 720, 720
16. N. Merlet and J. Zerubia. New Prospects in Line Detection by Dynamic Programming. *IEEE Transactions on Pattern Analysis and Machine Intelligence*, 18(4):426–431, 1996. 720

17. W. Neuenschwander, P. Fua, G. Székely, and O. Kübler. From Ziplock Snakes to Velcro<sup>TM</sup> Surfaces. In *Automatic Extraction of Man-Made Objects from Aerial and Space Images*, pages 105–114, Basel, Switzerland, 1995. Birkhäuser Verlag. 720, 726
18. R. Ruskoné and S. Airault. Toward an Automatic Extraction of the Road Network by Local Interpretation of the Scene. In *Photogrammetric Week*, pages 147–157, Heidelberg, Germany, 1997. Wichmann Verlag. 721, 721, 730
19. R. Ruskoné, L. Guigues, S. Airault, and O. Jamet. Vehicle Detection on Aerial Images: A Structural Approach. In *13th International Conference on Pattern Recognition*, volume III, pages 900–903, 1996. 721, 721, 730
20. S. Sarkar and K.L. Boyer. Integration, Inference, and Management of Spatial Information Using Bayesian Networks: Perceptual Organization. *IEEE Transactions on Pattern Analysis and Machine Intelligence*, 15(3):256–274, 1993. 722
21. C. Steger. An Unbiased Detector of Curvilinear Structures. *IEEE Transactions on Pattern Analysis and Machine Intelligence*, 20(2):113–125, 1998. 722, 722, 723, 725
22. C. Steger, H. Mayer, and B. Radig. The Role of Grouping for Road Extraction. In *Automatic Extraction of Man-Made Objects from Aerial and Space Images (II)*, pages 245–256, Basel, Switzerland, 1997. Birkhäuser Verlag. 721
23. G. Vosselman and J. de Knecht. Road Tracing by Profile Matching and Kalman Filtering. In *Automatic Extraction of Man-Made Objects from Aerial and Space Images*, pages 265–274, Basel, Switzerland, 1995. Birkhäuser Verlag. 720
24. A. Zlotnick and P.D. Carnine. Finding Road Seeds in Aerial Images. *Computer Vision, Graphics, and Image Processing: Image Understanding*, 57:243–260, 1993. 720